The gaseous content of the Blue Compact Galaxy Mrk 59

Alain Lecavelier des Etangs[1], Trinh X. Thuan[2], Yuri I. Izotov[3]

[1] *Institut d'Astrophysique de Paris, CNRS, 98bis Boulevard Arago, F–75014 Paris*
[2] *Astronomy Department, University of Virginia, Charlottesville, VA 22903*
[3] *Main Astronomical Observatory, National Academy of Sciences, 03680 Kyiv, Ukraine*

Abstract. *FUSE* far-UV spectroscopy of the nearby metal-deficient ($Z_\odot/8$) cometary Blue Compact Dwarf (BCD) galaxy Mrk59 have been used to investigate element abundances in its interstellar medium. The lack of diffuse H_2 ($N(H_2) \leq 10^{15} cm^{-2}$) is due to the combined effect of a strong UV radiation field and a low metallicity. By fitting the line profiles with multiple components having b = 7 km s^{-1} and spanning a radial velocity range of 100 km s^{-1}, we derive heavy element abundances in the neutral gas. We find log N(O I)/N(H I) = – 5.0±0.3, about a factor of 10 below the oxygen abundance of the supergiant H II region.

1 FUSE Observations of Mkr 59

The Blue Compact Dwarf (BCD) galaxy Markarian 59 (Mrk 59) ≡ I Zw 49 belongs to the class of cometary BCDs with an intense starburst at the end of an elongated low surface brightness stellar body. This BCD have numerous knots composed of a chain of H II regions, resulting from propagating star formation along the galaxy's elongated body and ending with the high-surface-brightness supergiant H II region. From deep ground-based spectrophotometric observations of the supergiant H II regions Noeske et al. (2000) derived an Oxygen abundance log O/H = -4.011 ± 0.003 ($Z_\odot/8$). O abundances were also derived for two other emission knots along the elongated body and were found to be the same within the errors. The small scatter in metallicity along the major axis of Mrk 59 ($\sim$ 0.2 dex) suggests that the mixing of elements in the ionized gas has been efficient on a spatial scale of several kpc.

Mrk 59 was observed during 7,865 s on 2000, January 11 with *FUSE* (Moos et al. 2000). The LWRS large entrance aperture (30"×30") was used, so that all of Mrk 59 which is $\sim$ 20" across (Noeske et al. 2000) is included within it.

Mrk 59 shows numerous interstellar absorption lines from the H I Lyman series (Ly β to Ly λ (H I 11)) and from other atoms and ions such as C II, C III, N I, N II, N III, O I, Si II, S III, S IV, Fe II and Fe III. Several stellar features such as the Si IV and S VI lines are also detected (Thuan et al. 2001a).

2 Narrow cores and broad wings of the H I Lyman series line profiles: interstellar and stellar absorption

We found that the shapes of the H I Lyman series lines cannot be reproduced with Voigt profiles characterized by a single H I column density. Damping

wings are clearly visible, signaling a very large H I column density $\sim 5 \times 10^{22}$ cm^{-2}. However, this high column density is not consistent with the shape of the strongest H I lines (Lyman β to Lyman δ). For instance, although damping wings are also present, the core of the Lyman δ line is thin and cannot be fitted with a model profile with the column density needed to fit the higher lines in the series. The thin core implies a smaller column density, of the order of 10^{21} cm^{-2}. We interpret that by a non-interstellar but stellar origin of the wide damping wings. We conclude that the broad wings of the above lines arise in the photospheres of numerous B stars, while their narrower cores are caused by interstellar absorption. By fitting the cores of the Lyman series lines, we obtain an interstellar H I column density of $\sim 7{\times}10^{20}$ cm^{-2}.

3 Upper limits on the diffuse H_2 content of Mrk 59

No line of H_2 is seen at the radial velocity of Mrk 59. Using nine H_2 Lyman bands (0–0 to 8–0), we conclude that the total column density of diffuse H_2 is $\leq 10^{15}$cm^{-2}. This implies that the ratio of H_2 to HI is $\leq 10^{-6}$. The corresponding average molecular fraction $f{=}2N(H_2)/(N(\text{H I}){+}2N(H_2))$ is $\leq 3 \times 10^{-6}$.

By calculating the amount of H_2 molecules formed on the surface of dust grains, we find that the expected $N(H_2)$ must be $\sim 2{\times}10^{12}$ cm^{-2}, consistent with our upper limit. As compared to the Milky Way, the low column density of diffuse H_2 in Mrk 59 is due to the combined effects of a large UV flux which destroys the H_2 molecules and of a low metallicity resulting in a scarcity of dust grains on which H_2 form (see the full discussion in Thuan et al. 2001a).

4 Heavy element abundances

To estimate the abundances, we consider two cases. The first case presented during the meeting assumes that there is a single velocity component along the thousands of lines of sight to the stars of Mkr 59. In this case, absorption lines that are broader than the instrumental Point Spread Function and do not go down to zero are supposed to be not saturated. The second case, suggested during the meeting (York, public communication), assume multiple velocity components along the multiple lines of sight, some of which may have saturated profiles.

4.1 Profile fitting with a single velocity component

We consider first the single interstellar velocity component case. Some of the lines, like the Fe III and S III lines, are very broad with unreasonably large Doppler widths ($b{\geq}100$ km s^{-1}), suggesting, as for the H I lines, that these metal lines have some contamination by stellar absorption. The resulting column densities ($\log N_1$) and Doppler widths (b_1) along with their error bars are given in Table 1. The error bars of the column densities include the uncertainty

Table 1: Heavy element column densities in Mrk 59

	b_1[a]	log N_1[a]	log N_2[b]		b_1[a]	log N_1[a]	log N_2[b]
C III	≤ 35	18.4±0.1	18.2±0.1	N I	40±20	$14.0^{+0.3}_{-0.4}$	$14.6^{+0.4}_{-0.3}$
N II	30±10	$14.2^{+0.1}_{-0.2}$	$15.1^{+2.2}_{-0.8}$	O I	40±20	$15.1^{+0.3}_{-0.3}$	$15.8^{+0.3}_{-0.3}$
S III	95±15	15.1±0.1	$19.0^{+0.1}_{-0.2}$	S IV	30±10	$14.2^{+0.1}_{-0.2}$	$14.9^{+0.9}_{-0.6}$
Fe II	40±15	$13.9^{+0.1}_{-0.2}$	$14.4^{+0.3}_{-0.3}$	Fe III	105±10	15.1±0.1	$18.9^{+0.1}_{-0.1}$

a)Fitting with a single Voigt profile. b_1 is in km s^{-1}. Error bars are 3 σ limits.
b)Fitting with multiple velocity components, each with b_2 = 7 km s^{-1}, and spanning a velocity range of 100 km s^{-1}. Error bars are 2 σ limits.

in b. These abundances of the metals relative to N(H I) are extremely low. In particular, with log N(O I)/N(H I) = – 5.7, the oxygen abundance in the H I gas could be $\sim$ 50 times lower than the oxygen abundance in the ionized gas, as determined from the optical emission line spectrum of the supergiant H II region in Mrk 59. However, these very low abundances may be underestimates due to the saturation of some lines of sight.

4.2 Profile fitting with multiple velocity components

We are observing through the *FUSE* aperture along thousands of lines of sight towards UV-bright stars. The observed spectrum is the sum of many spectra. It can happen that some lines of sight have saturated absorption lines with a small b parameter, but because they have different radial velocities spread over several tens of km s^{-1}, the broad absorption line resulting from the sum of many narrow absorption lines does not go to zero intensity, and its width is larger than the Point Spread Function. In that case, a single velocity component fit to the line profile would result in an overestimate of the b parameter and in an underestimate of the column density.

To investigate this issue, we have calculated profiles resulting from the addition of multiple lines of sight. We adopt the simple model where the different lines of sight have radial velocities distributed uniformly between $v_{\rm Mrk59} - \Delta v/2$ and $v_{\rm Mrk59} + \Delta v/2$, where Δv is the spread in velocity due mostly to the velocity dispersion of the system of absorbing clouds along the multiple lines of sight, and also partly to the wavelength smearing caused by the extension of Mrk 59 within the aperture. We determine the best estimates of b (assumed to be the same for all lines of sight) and Δv by the simultaneous fit of several lines of O I, N I and Fe II. Each of these elements having several transitions with different oscillator strengths, this well constrains b and Δv to reasonable values: b=7^{+13}_{-3} km s^{-1} and Δv=100±20 km s^{-1} (2σ limits, see Fig 1). Note that the value of Δv is very close to the FWHM of 92 km s^{-1} of the H I profile (Thuan et al. 2001b). The heavy element column densities derived with the multi-component fit are given in Table 1 (log N_2). Those are larger than in the case of a single component fit, by a mean factor of $\sim$5. The very large column densities derived for C III, S III and Fe III are caused by

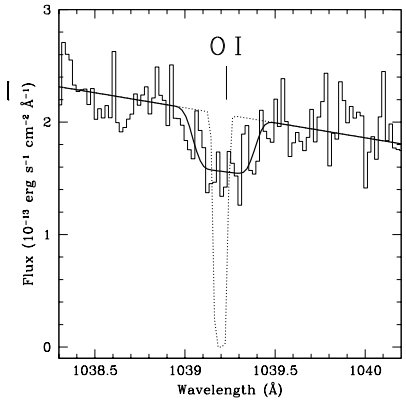

Figure 1: Fit to the O I 1039Å absorption line with a column density N(O I) = 7×10^{15}cm^{-2}. The fit is obtained by the addition of multiple profiles. Δv and b parameters are constrained by the simultaneous fit of several lines of O I, N I and Fe II. The thick solid line gives the resulting fit to the data with Δv = 100 km s^{-1} and b = 7 km s^{-1}. The dotted line represents an example of one line of sight with b = 7 km s^{-1}. With this column density, such an individual line of sight is saturated and goes down to the zero intensity level. However the absorption line resulting from the addition of many narrower profiles does not go to the zero intensity level, although it is broader than the width of the instrumental Point Spread Function ($\sim$ 0.1Å).

stellar contamination. It is interesting to note that, even with a higher derived oxygen abundance, log N(O I)/N(H I) = – 5.0±0.3, the H I absorbing cloud still has a metallicity lower than that of the supergiant H II region by a factor of $\sim$ 10. This suggests self-contamination of the H II region by heavy elements released during the present burst of star formation (Kunth & Sargent 1986). While mixing of these newly formed heavy elements appears to have occurred on the scale ($\sim$ 2 kpc) of the H II regions (Noeske et al. 2000), it has not had time to occur for the whole neutral gas component as the H I envelope surrounding the star-forming regions is much more extended (its diameter is $\sim$ 19 kpc from the VLA map by Thuan et al. 2001b).

Acknowledgements. The profile fitting was done using the Owens procedure developed by Dr. M. Lemoine and the *FUSE* French Team. We warmly thank Dr. D. York for his important suggestion during the meeting.

References

[1] Kunth, D. & Sargent, W.L.W. 1986, ApJ 300, 496
[2] Moos, H.W. et al. 2000, ApJ , 538, L1
[3] Noeske K. G., et al., 2000, A&A , 361, 33
[4] Thuan T. X., Lecavelier A., & Izotov Y. I. 2001a, ApJ submitted
[5] Thuan, T. X., Lévrier, F., & Hibbard, J. E. 2001b, ApJ in preparation